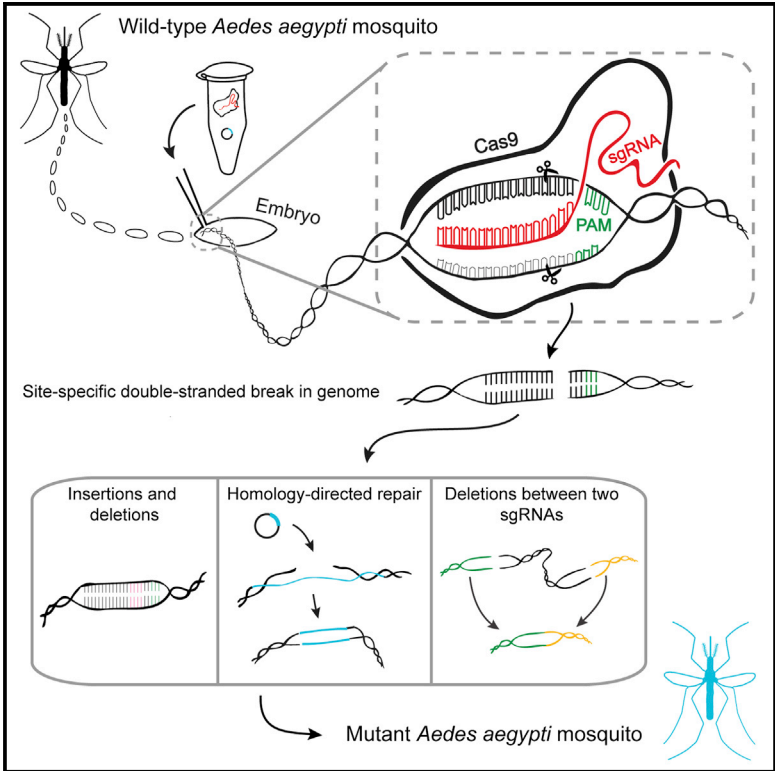


# Cell Reports

## Genome Engineering with CRISPR-Cas9 in the Mosquito *Aedes aegypti*

### Graphical Abstract



### Authors

Kathryn E. Kistler, Leslie B. Vosshall, Benjamin J. Matthews

### Correspondence

ben.matthews@rockefeller.edu

### In Brief

The mosquito *Aedes aegypti* is responsible for infecting hundreds of millions of humans with life-threatening diseases each year. Kistler et al. show that CRISPR-Cas9 can be used to engineer precise loss-of-function mutations and targeted integration of exogenous sequences, enabling detailed genetic study of this deadly disease vector.

### Highlights

- CRISPR-Cas9 is an effective tool for genome editing in the mosquito *Aedes aegypti*
- Injection mixtures and sgRNAs are optimized to yield high survival and editing
- Single- and double-stranded DNA donors can precisely integrate into the genome
- Genome editing results in stable germline transmission of mutant alleles

### Accession Numbers

PRJNA272452



# Genome Engineering with CRISPR-Cas9 in the Mosquito *Aedes aegypti*

Kathryn E. Kistler,<sup>1</sup> Leslie B. Vosshall,<sup>1,2</sup> and Benjamin J. Matthews<sup>1,2,\*</sup><sup>1</sup>Laboratory of Neurogenetics and Behavior, The Rockefeller University, 1230 York Avenue, New York, NY 10065, USA<sup>2</sup>Howard Hughes Medical Institute, 1230 York Avenue, New York, NY 10065, USA\*Correspondence: [ben.matthews@rockefeller.edu](mailto:ben.matthews@rockefeller.edu)<http://dx.doi.org/10.1016/j.celrep.2015.03.009>This is an open access article under the CC BY-NC-ND license (<http://creativecommons.org/licenses/by-nc-nd/4.0/>).

## SUMMARY

The mosquito *Aedes aegypti* is a potent vector of the chikungunya, yellow fever, and dengue viruses, responsible for hundreds of millions of infections and over 50,000 human deaths per year. Mutagenesis in *Ae. aegypti* has been established with TALENs, ZFNs, and homing endonucleases, which require the engineering of DNA-binding protein domains to provide genomic target sequence specificity. Here, we describe the use of the CRISPR-Cas9 system to generate site-specific mutations in *Ae. aegypti*. This system relies on RNA-DNA base-pairing to generate targeting specificity, resulting in efficient and flexible genome-editing reagents. We investigate the efficiency of injection mix compositions, demonstrate the ability of CRISPR-Cas9 to generate different types of mutations via disparate repair mechanisms, and report stable germline mutations in several genomic loci. This work offers a detailed exploration into the use of CRISPR-Cas9 in *Ae. aegypti* that should be applicable to non-model organisms previously out of reach of genetic modification.

## INTRODUCTION

As a primary vector of the serious and sometimes fatal chikungunya, yellow fever, and dengue viruses, the mosquito *Aedes aegypti* (*Ae. aegypti*) is responsible for hundreds of millions of human infections annually (Bhatt et al., 2013). To transmit disease, a female mosquito must bite an infected individual, and, after a period of viral incubation within the mosquito, bite and infect another human. Female mosquitoes use cues such as odor, carbon dioxide, and temperature to locate a host and obtain a blood-meal (McMeniman et al., 2014), which is used to produce a clutch of approximately 100 eggs. Once a mosquito has developed mature eggs, she uses volatile and contact cues to locate and evaluate a body of water at which to lay her eggs. Our long-term goal is to use genome-engineering techniques coupled with quantitative behavioral analysis to investigate the genetic and neural bases of innate chemosensory behaviors in this important disease vector.

Clustered regularly interspaced palindromic repeats (CRISPR) and CRISPR-associated (Cas) genes are components of an adaptive immune system that are found in a wide variety of bacteria and archaea (Doudna and Charpentier, 2014). Beginning in late 2012 (Jinek et al., 2012), the bacterial type II CRISPR-Cas9 system was adapted as a genome-engineering tool in many different organisms and in vitro preparations, dramatically expanding the ability to modify genomes (Doudna and Charpentier, 2014). The ease of designing and generating these reagents at the bench has opened the door for studies of gene function in non-traditional model organisms.

The genome of *Ae. aegypti* is relatively large and incompletely mapped (Juneja et al., 2014; Nene et al., 2007; Timoshevskiy et al., 2014), making it difficult to recover mutations generated by traditional forward genetics. *Ae. aegypti* has a recent history of genetic modification, including transposon-mediated transgenesis (Coates et al., 1998; Lobo et al., 2002) and loss-of-function gene editing with zinc-finger nucleases (ZFNs) (DeGennaro et al., 2013; Liesch et al., 2013; McMeniman et al., 2014), TAL-effector nucleases (TALENs) (Aryan et al., 2013a, 2014), and homing endonuclease genes (HEGs) (Aryan et al., 2013b). ZFNs and TALENs are modular DNA-binding proteins tethered to a non-specific FokI DNA nuclease (Carroll, 2014), while HEGs are naturally occurring endonucleases that can be reengineered to target novel sequences (Stoddard, 2014). Targeting specificity by these reagents is conferred by context-sensitive protein-DNA-binding interactions, and these proteins can be difficult to engineer.

Here we describe methods for site-directed mutagenesis in *Ae. aegypti* using RNA-guided endonucleases based on the type II CRISPR-Cas9 system. The double-stranded endonuclease Cas9 derived from *Streptococcus pyogenes* uses RNA-DNA Watson-Crick base-pairing to target to specific genomic locations. This system has been adapted for precision genome engineering in dozens of organisms from bacteria to primates (Doudna and Charpentier, 2014; Peng et al., 2014). In particular, two studies in the vinegar fly *Drosophila melanogaster* (Bassett et al., 2013) and the zebrafish *Danio rerio* (Hwang et al., 2013) were important in guiding our early attempts to adapt CRISPR-Cas9 to *Ae. aegypti*.

A detailed bench manual with step-by-step guidance for designing, generating, and testing these reagents in mosquitoes is available as [Data S1](#). Given the proven flexibility of this system, we believe that the protocols and procedures outlined here and by numerous other laboratories will continue to be optimized and modified for use in many organisms for which precision genome engineering has not yet been employed.

## RESULTS

### Outline of CRISPR-Cas9 System and Injection Components

The core of the CRISPR-Cas9 system has two components as follows: (1) a synthetic single guide RNA (sgRNA), which is a small RNA containing 17–20 bases of complementarity to a specific genomic sequence; and (2) the Cas9 nuclease derived from *Streptococcus pyogenes* (SpCas9). SpCas9 forms a complex with the sgRNA and induces double-stranded DNA breaks at sequences of the genome that are directly 5' to a protospacer-adjacent motif (PAM) and are complementary to the sgRNA recognition site. The PAM sequence for SpCas9 is NGG, which occurs approximately once every 17 bp in the *Ae. aegypti* genome, making it possible to target essentially any locus. All work in this paper utilizes SpCas9, which is henceforth referred to simply as Cas9.

To generate stable germline mutations, CRISPR-Cas9 reagents are injected into pre-blastoderm-stage embryos composed of a syncytium of nuclei prior to cellularization that offers access of genome-editing reagents to the nuclei of both somatic and germline cells. Embryos are microinjected 4–8 hr after egg laying, and allowed to develop for 3 days before being hatched in a deoxygenated hatching solution (Lobo et al., 2006). G<sub>0</sub> pupae are collected for sequencing to determine genome modification rates, or are allowed to emerge as adults and outcrossed to wild-type LVP-IB12 mosquitoes. Following blood-feeding, G<sub>1</sub> eggs are collected from these outcrosses to screen for germline transmission of stable mutations.

When faced with a double-stranded DNA break, DNA repair machinery can resolve this break in one of two ways as follows: (1) non-homologous end joining, which can result in small insertions and deletions; or, less frequently, (2) homology-directed repair, which uses exogenous sequences containing regions of homology surrounding the cut site as a template for repair. Cutting with multiple sgRNAs can result in large deletions between the two cut sites. In this paper, we discuss stable germline transmission of all three types of alleles in *Ae. aegypti*.

### Identifying Optimal Injection Mixes for CRISPR-Cas9 Mutagenesis

Insertions and deletions resulting from non-homologous end joining are a proxy for the activity of a particular sgRNA/Cas9 combination and can be detected by Surveyor or T7 Endonuclease I (T7E1) (Reyon et al., 2012), high-resolution melting point analysis (HRMA) (Dahlem et al., 2012), Sanger sequencing (Brinkman et al., 2014), or deep sequencing (Gagnon et al., 2014). Each of these techniques evaluates the level of polymorphism in a short PCR-generated amplicon surrounding the sgRNA target site. With the exception of deep sequencing, these approaches provide only semiquantitative estimates of the mutagenesis in each sample, and, furthermore, HRMA and Surveyor/T7E1 are prone to false positives because the *Ae. aegypti* genome is highly polymorphic.

We used deep sequencing of barcoded PCR amplicons surrounding putative CRISPR-Cas9 cut sites from small pools of injected animals to accurately determine the rates of cutting at

different genomic loci. Sequencing libraries were prepared using a two-step PCR process that incorporates adaptor and barcode sequences necessary for Illumina sequencing (Figure 1A). To minimize the underestimation of mutagenesis rate due to deleted primer-binding sequences, we designed a forward primer 50–100 bp from the predicted sgRNA cut site and a reverse primer >50 bp on the opposite side. We estimated that 10,000–100,000 reads per sample were ample for this analysis, so sequencing of amplicons from three sgRNAs per gene, for ten different genes, costs approximately \$70 per gene at current pricing (MiSeq v3 reagents, 150-cycle flowcell, item MS-102-3001). In our judgment, this method is cost-effective and provides high resolution relative to all other techniques.

Following sequencing, reads were aligned to a reference sequence using the GSNAP short read aligner (Wu and Nacu, 2010), and analyzed with the python package pysamstats. This procedure reveals the number of polymorphisms, including insertions and deletions, found in reads that span each nucleotide of a reference sequence (Figure 1B). In injections containing a sgRNA and Cas9, a pattern of elevated insertions and deletions can be observed with a peak 3 bp 5' of the beginning of the PAM, exactly the position at which Cas9 is known to make a double-stranded break (Figure 1C). Importantly, there was high concordance in the mutagenesis rates among multiple biological replicates (Figure 1C).

We next varied the delivery method and concentration of Cas9, and the concentration of a given sgRNA, to determine an optimal injection mix. A DNA plasmid that expresses Cas9 under the control of the *Ae. aegypti* polyubiquitin (PUB) promoter did not induce detectable rates of insertions or deletions with a validated sgRNA (data not shown). When included at 500 ng/μl, both Cas9 mRNA and recombinant Cas9 protein induced detectable mutagenesis at two distinct guide RNA sites. However, Cas9 protein induced mutagenesis at rates five to ten times higher than Cas9 mRNA (Figure 1D). To test whether the concentration of sgRNA or Cas9 mRNA or protein was limiting in these earlier injections, we tried four additional injection mixes with a single validated sgRNA (Figure 1E), and determined that mixes containing 400 ng/μl Cas9 recombinant protein induced the highest rates of mutagenesis. Increasing sgRNA concentration did not dramatically increase mutagenesis rates.

### Identifying Active sgRNAs for a Given Genomic Target

We reasoned that sgRNAs causing higher somatic cut rates would be more likely to result in stable germline mutations. We manually searched six different genes for sgRNAs composed of 17–20 bases (Fu et al., 2014) adjacent to a PAM and beginning with GG or G to facilitate in vitro transcription. We then selected three sgRNAs per gene with a low probability of off-target binding (Figure 2A; Table S1).

To test the efficiency of these sgRNAs, we performed a series of six small test injections of recombinant Cas9 protein at 333 ng/μl and a pool of three sgRNAs (40 ng/μl each), each targeting a different gene, into 145–168 *Ae. aegypti* embryos (Figure 2B). Survival rates were very high for these injections (ranging from 46.1%–63.3%, as compared to 18.6% average survival with 500 ng/μl Cas9 protein or mRNA). We attribute this marked increase in survival to the reduction in Cas9 concentration.

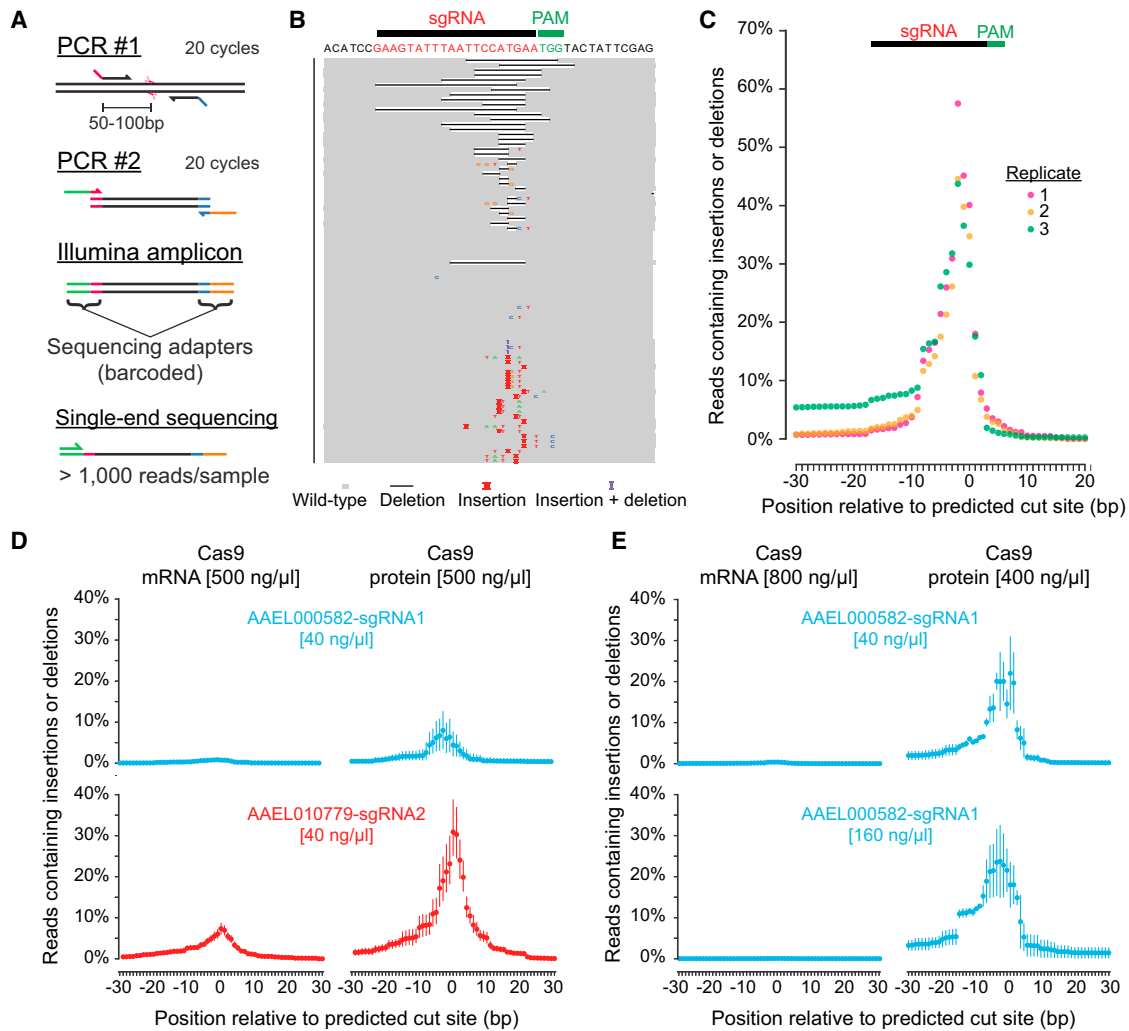


**Figure 1. Deep Sequencing to Quantify CRISPR-Cas9 Efficiency**

(A) Schematic of PCR amplicon barcoding.

(B and C) Amplicons generated from adults reared from embryos injected with 333 ng/ $\mu$ l Cas9 protein and 40 ng/ $\mu$ l sgRNA (AAEL004091-sgRNA1) using primers AAEL004091-1-F and AAEL004091-1-R. (B) Visualization of a subset of alignments to the amplicon reference sequence (top) and (C) quantification of three replicate libraries as percentage of reads aligned to a given base that contain an insertion or deletion at that base.

(D and E) Summary of sequencing data from animals injected with two different sgRNAs in combination with Cas9 mRNA (left) or Cas9 recombinant protein (right), at the indicated concentrations; n = 7–18 libraries (D) and n = 2 libraries (E). Data are plotted as mean (circle) and 95% confidence intervals (line).

Surviving embryos were reared to pupal stages and collected for sequencing of PCR amplicons (Figure 2B).

All 18 sgRNAs induced detectable levels of mutagenesis, which varied within and among different genomic targets (Figure 2C), reflecting sequence- or context-dependent effects on sgRNA efficiency that are not yet fully understood. Designing and testing three sgRNAs resulted in the identification of at least one highly active sgRNA for the six genomic targets tested here. Users are strongly advised to test multiple sgRNAs per gene before undertaking large-scale mutagenesis injections.

### Germline Transmission of Mutant Alleles

We next examined whether somatic mutagenesis detected in adults reared from injected embryos ( $G_0$  animals) resulted in

the transmission of stable mutant alleles through the germline to their offspring ( $G_1$  animals). We designed an sgRNA near the 5' end of *Aeeg-wtrw*, and included 300 ng/ $\mu$ l of a 200-bp single-stranded DNA oligodeoxynucleotide (ssODN) donor as a template for homology-directed repair. The ssODN had homology arms of 87–90 bases on either side of the Cas9 cut site, flanking an insert with stop codons in all three frames of translation and a restriction enzyme site. Successful integration of this template would truncate the full-length protein of 908 amino acids at 91 amino acids (Figure 3A).

Embryos (n = 636) were injected with a mixture of 200 ng/ $\mu$ l Cas9 mRNA and 12.5 ng/ $\mu$ l sgRNA (these injections were performed prior to the optimization of injection mixes described above). We performed amplicon sequencing on six pools of

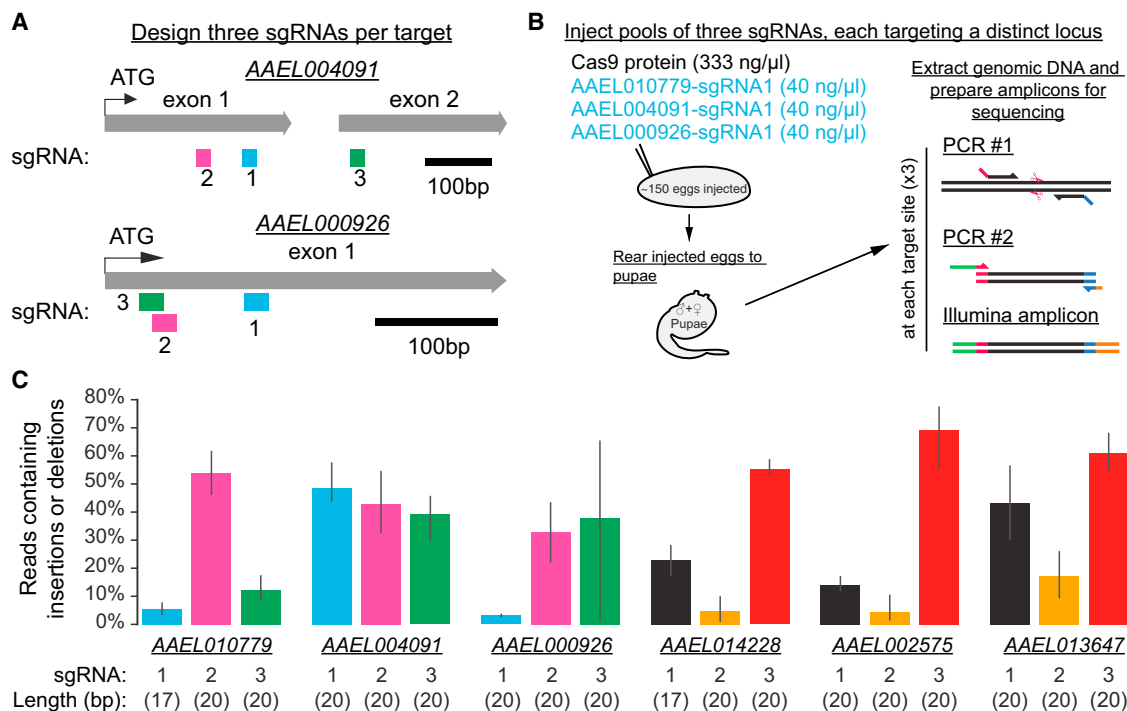


**Figure 2. Identifying Active sgRNAs**

(A) Schematic of two target genes in the *Ae. aegypti* genome indicating the three sgRNAs designed in the first exon of each gene. (B) Schematic of the workflow for a small injection (approximately 150 embryos) of Cas9 protein and a pool of three sgRNAs against three distinct target genes. (C) Sequencing results from six small injections (sgRNA sequences can be found in Table S1); n = 3 sequencing libraries per sgRNA. Data are presented as means and 95% confidence intervals.

five to six adult  $G_0$  animals after they were outcrossed and allowed to lay eggs (Figure 3B). These samples contained a maximum mutation rate of 24.87% centered on the Cas9 cut site (Figure 3C). Amplicons derived from animals injected with an sgRNA targeting a different region of the genome contained no detectable insertions or deletions at the *Aaeg-wtrw* locus (Figure 3C). On average 0.71% of aligned reads from six samples contained sequences corresponding to the single-stranded DNA donor (Figure 3D), indicating that the ssODN template could drive homology-directed repair in somatic tissue, albeit at a much lower frequency than insertions or deletions mediated by non-homologous end joining.

To determine whether these mutations were stably transmitted through the germline, we sequenced PCR amplicons derived from 62 pools each containing five male and five female  $G_1$  offspring. Analysis of resulting insertions and deletions using the Genome Analysis Toolkit [GATK (DePristo et al., 2011)] revealed at least 117 mutant chromosomes spread across 50 pools. Given that each  $G_1$  individual can only carry a single mutant chromosome, we concluded that the  $G_1$  mutation rate was at least 117/620 or 18.9% (Figure 3E). Four of these alleles corresponded perfectly to the sequence of the ssODN, so our rate of stable germline transmission of alleles generated by homology-driven repair was at least 0.6% (Figure 3E). This is similar to rates in  $G_0$  animals (Figures 3D and 3E), suggesting that somatic mutagenesis can predict the efficiency of germline mutagenesis.

We hatched  $F_2$  eggs from a single family containing an allele generated by homology-directed repair. Sequencing of single-pair crosses allowed us to isolate a stable mutant line that could be genotyped by the ssODN-introduced restriction site (Figure 3F). This line was outcrossed for eight generations to wild-type mosquitoes to increase genetic diversity and reduce the possibility of retaining off-target mutations. The presence of the mutant allele was verified in individual female mosquitoes at each generation by molecular genotyping, and eggs were hatched from heterozygous mutant females only.

### Deletions Induced by Multiplexed sgRNAs

Double-stranded breaks induced at multiple sgRNA sites can induce large deletions between the two cut sites in *D. melanogaster* (Ren et al., 2013). We performed a series of five injections into small numbers of embryos using sgRNAs targeting three different genes. All but one of these sgRNAs (AAEL000926-sgRNA4) was validated previously (Figure 2C), and injection mixes also included ssODN donors (Figure 4A; Data S2).  $G_1$  embryos were hatched and screened as individual families derived from a single female  $G_0$  (Figure 4B). We identified mutant families by screening PCR amplicons generated from pools of  $G_1$  male pupae for size-shifted bands. Following outcrossing and egg collection, individual  $G_1$  females were similarly genotyped by PCR amplicon size (Figures 4C–4E) to estimate mutation rates.



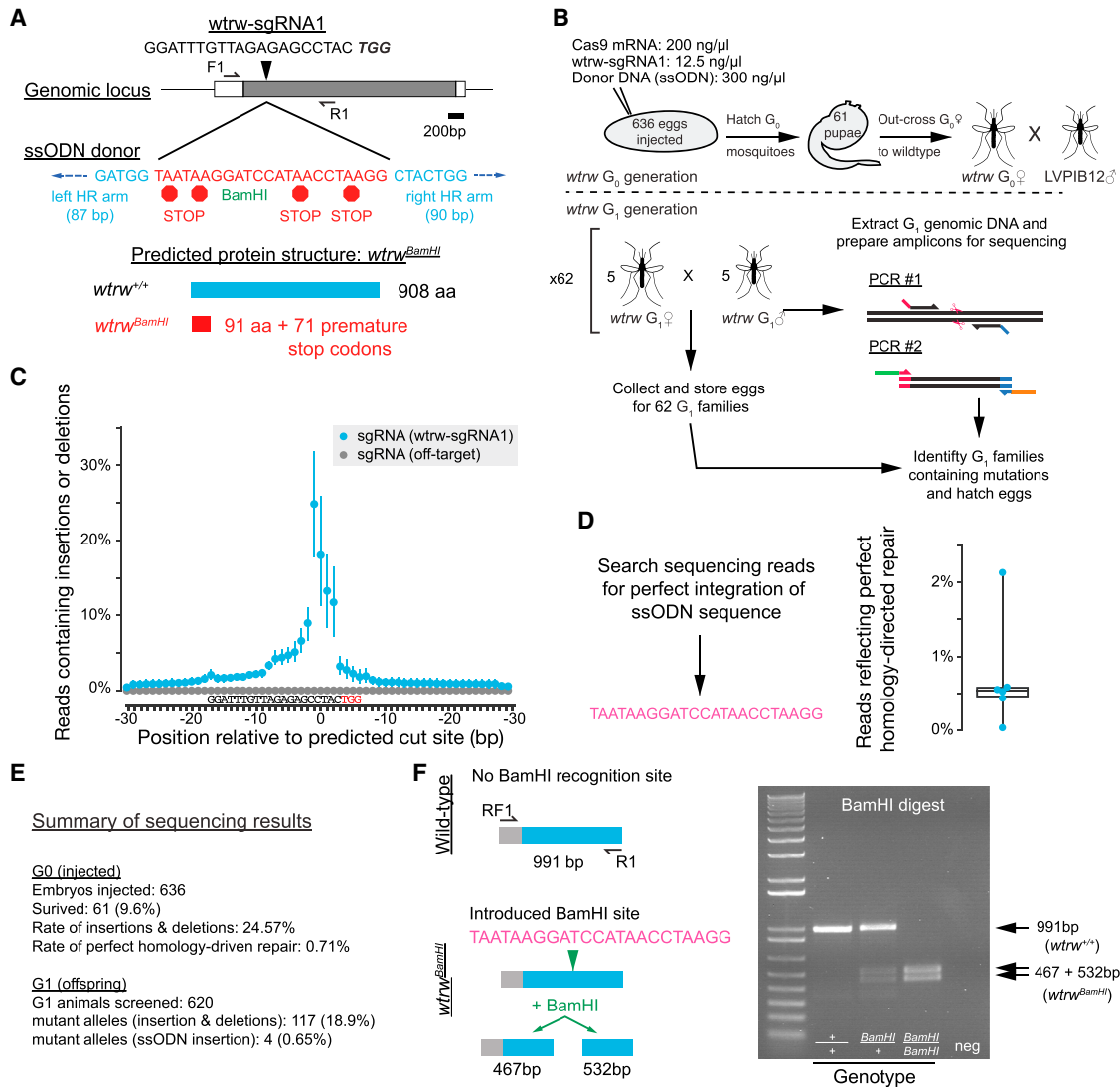


**Figure 3. Germline Transmission of Mutant Alleles**

(A) Schematic of the *Ae. aegypti wtrw* locus, detailing the sgRNA-binding site, ssODN donor, and modified locus.

(B) Schematic of injection performed to isolate mutations.

(C) Summary sequencing data from G<sub>0</sub> adults; n = 6 (*wtrw*) and n = 3 (off-target), presented as means (circle) and 95% confidence intervals (lines).

(D) Exogenous ssODN sequence that was used as a query for the unix tool grep (left) and reads containing perfect homology-directed repair presented as a boxplot (right, box represents median and first and third quartiles, whiskers represent data range).

(E) Summary of G<sub>0</sub> and G<sub>1</sub> sequencing results.

(F) Restriction enzyme diagnostic of ssODN insertion.

We found a wide range of mutant transmission rates in families derived from single G<sub>0</sub> individuals (Figure 4D). Sanger sequencing of some bands revealed that mutations ranged from simple deletions, to homology-directed repair from the ssODN donor, to more complex modifications, including polymorphisms, inversions, and duplications. Additionally, we were successful in obtaining germline mutations at high rates in each of three small injections (Figure 4E), making this a cost-effective and efficient way to generate loss-of-function mutant alleles. The relatively large size of deletions generated by this method simplifies sized-based molecular genotyping of females at each generation.

### Integration and Transmission of Large Fluorescent Cassettes

Finally, we asked whether CRISPR-Cas9 could be used to introduce gene cassettes via homology-dependent repair. Previously, ZFNs were used to introduce large cassettes into *Ae. aegypti* from a plasmid DNA donor with homology arms of at least 800 bp on either side (Liesch et al., 2013; McMeniman et al., 2014), generating a null mutant by the insertion of a visible fluorescent reporter. We performed injections with Cas9 protein, a validated sgRNA, and a plasmid donor containing homology arms of 799 bp and 1,486 bp. This plasmid (Addgene 47917)

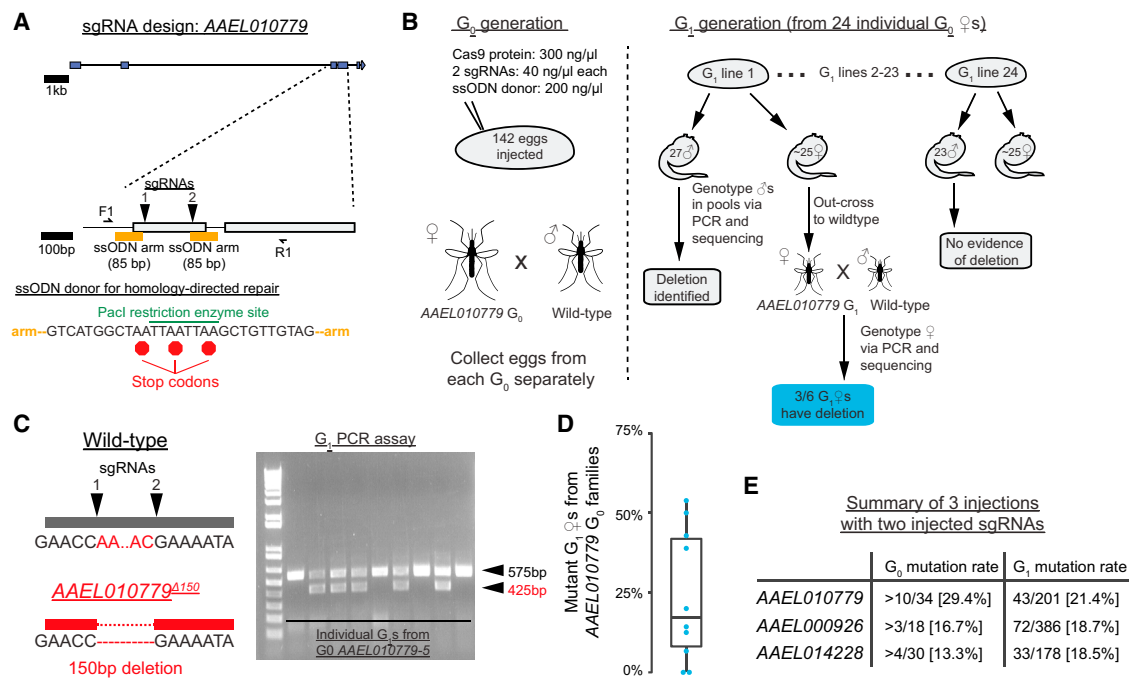


**Figure 4. Deletions Generated by Multiple sgRNAs**

(A) Schematic of the *AEEL010779* genomic locus, detailing the design of two sgRNAs and an ssODN donor.

(B) Injection strategy to identify deletion events in  $G_1$  animals with the injection of a small (125–150) number of embryos.

(C) Example agarose gel of nine  $G_1$  female offspring of a single  $G_0$  female reveals four wild-type and five heterozygous individuals.

(D) Percentage of mutant *AEEL010779*  $G_1$  females from the ten  $G_0$  families identified as containing at least one mutant allele is presented as a boxplot (box represents median and first and third quartiles, whiskers represent data range).

(E) Summary data of  $G_1$  mutagenesis from three injections of this type.

contains a cassette comprising the constitutive PUB promoter driving the expression of the fluorescent reporter ECFP (Figures 5A and 5B). Arms were cloned from wild-type LVP-IB12 mosquitoes and were designed to avoid repetitive sequences such as transposable elements. Following injection, individual female  $G_0$  animals were outcrossed to wild-type mosquitoes and  $G_1$  eggs were collected (Figure 5A). Because we previously observed that successful homology-directed repair occurs primarily, if not exclusively, in female  $G_0$  *Ae. aegypti*, we discarded  $G_0$  males and screened  $G_1$  families generated from females.

$G_1$  larvae at 3–5 days post-hatching were screened under a fluorescence dissecting microscope for the fluorescent protein expressed under control of the PUB promoter (Figure 5C). Fluorescent individuals were collected, reared to adulthood, and crossed to wild-type animals to establish stable lines. To verify gene-specific insertion of our cassette, we designed PCR primers spanning both homology arms (Figure 5C). It is critical that these primers are designed outside each arm and that bands obtained are sequenced to verify junctions between genomic and exogenous sequence on each end of the insertion.

Lines containing verified targeted insertions were outcrossed to wild-type mosquitoes for eight generations by selecting fluorescent larvae and pupae. A homozygous line was established by mating heterozygotes. Putative homozygous mosquitoes were selected by increased fluorescence as larvae, separated

by sex, and used to establish single-pair matings. The genotype of these single-pair matings was verified by PCR (Figure 5D).

We generated verified targeted insertions in two of four genomic loci with the *Ae. aegypti* PUB promoter driving the expression of ECFP (Figure 5; Table S3) or dsRed (Table S3), suggesting that homology-directed repair with large plasmid donors occurs at a relatively low frequency compared to other forms of CRISPR-Cas9-mediated genome modification. A drastic variance in the efficiency noted in two injections (Table S3) suggests that simple modifications of injection mix component concentration may increase integration rates, perhaps at the expense of embryo survival. The identification of stably transmitting integration events at non-targeted genomic loci underscores the necessity of verifying all lines generated by this technique by PCR or other molecular methods.

## DISCUSSION

We have demonstrated that the CRISPR-Cas9 system is a highly effective tool for precision genome editing in the mosquito *Ae. aegypti*. Compared to the relatively low throughput and high cost of ZFN- and TALEN-mediated mutagenesis, the ease of designing and producing CRISPR-Cas9 reagents has allowed us to generate stable and precise loss-of-function mutations in five genes described here. A variety of mutant alleles can be recovered, including frameshift mutations caused by insertions

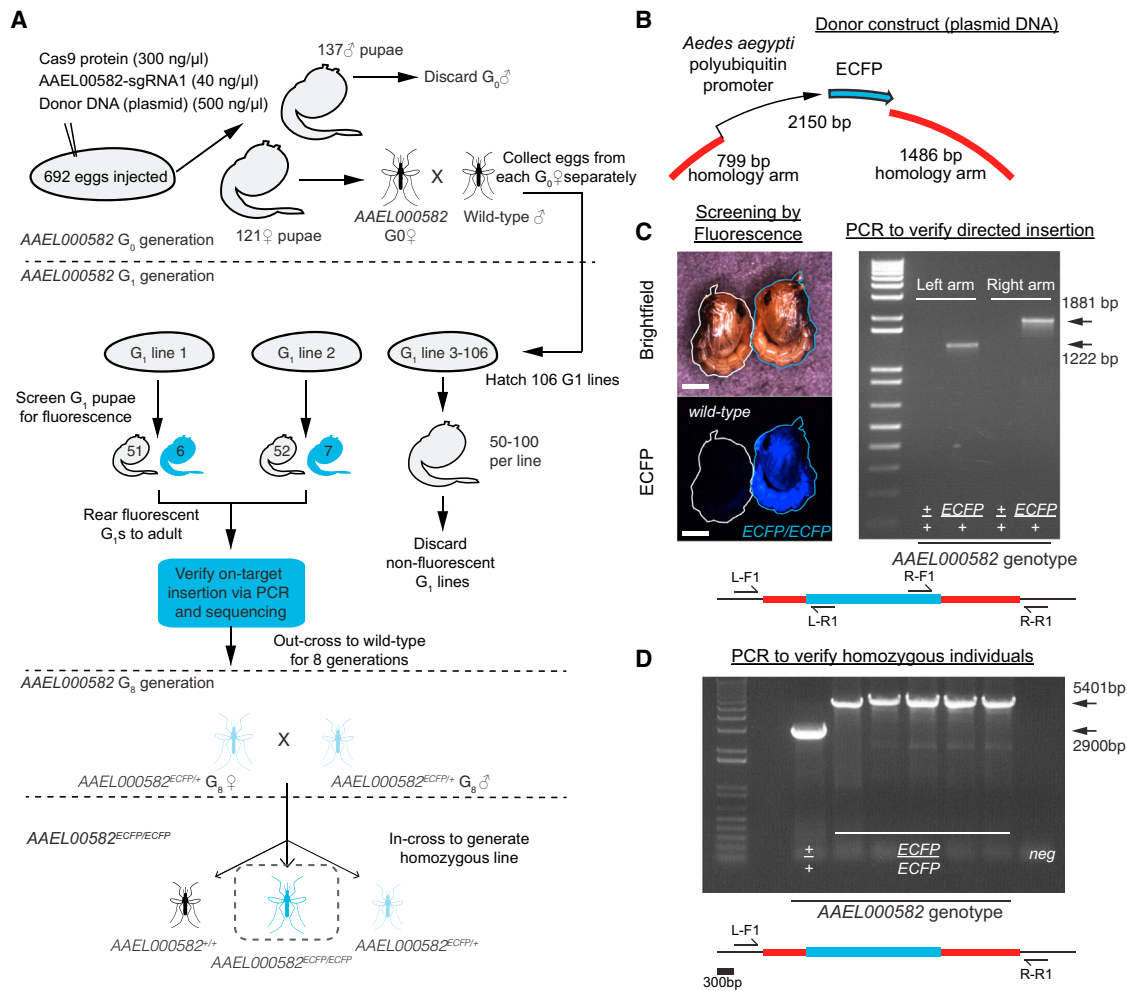


**Figure 5. Insertion of Fluorescent Cassettes by Homology-Directed Repair**

(A) Schematic of injection and screening strategies to obtain alleles with an insertion of an ECFP cassette (blue).

(B) Design of the plasmid donor.

(C) At left, bright-field and ECFP fluorescence images of two pupae: wild-type (top) and AAEL000582<sup>ECFP/ECFP</sup> (bottom); scale bar, 1 mm. At right and below, PCR strategy to verify directed insertion of the PUB-ECFP cassette.

(D) PCR strategy to identify homozygous individuals. See also Table S3.

or deletions, deletion of a region between two sgRNA target sites, and integration of exogenous sequences from a single-stranded oligonucleotide or a double-stranded plasmid DNA donor. This protocol provides a step-by-step manual to mutagenesis in *Ae. aegypti* and also provides general principles that will be useful when translated to other species.

### Optimal Injection Mix

We recommend recombinant Cas9 protein for its reproducibility, increased rates of mutagenesis, and embryo survival. It is likely more stable than mRNA, both at the bench and in injected embryos, and may form a complex with sgRNA in vitro prior to injection. This can stabilize sgRNA/Cas9 complexes (Jinek et al., 2014) and ensures mutagenesis without the delay of translation of Cas9 mRNA in the embryo. The specific concentrations suggested here represent a good trade-off between survival and efficiency in our

hands. However, further modifications to this protocol may result in significant increases in certain types of repair.

We recommend the following injection mix for *Ae. aegypti* embryos (this may be a good starting point for other insect embryos): 300 ng/ $\mu$ l recombinant Cas9 protein; 40 ng/ $\mu$ l sgRNA (each); and 200 ng/ $\mu$ l ssODN or 500 ng/ $\mu$ l double-stranded plasmid DNA (optional).

### Designing Active sgRNAs

As in other organisms and cell lines (Fu et al., 2014; Ren et al., 2014), we observed success with sgRNAs ranging in length from 17 to 20 bp. However, different sgRNAs varied significantly in effectiveness, even when targeted to a small region of the same gene (Figure 2). Additionally, a single genomic target (AAEL001123) was resistant to mutagenesis with six different sgRNAs. Further experiments will determine whether



sgRNA base composition (such as GC content) (Ren et al., 2014) or underlying chromatin state (Wu et al., 2014) influence efficacy. To maximize the chance of successful mutagenesis, we recommend designing and testing multiple sgRNAs targeting a given gene before committing to large-scale injections.

### Off-Target Effects

Off-target effects are a concern with any genome-editing technology, and we addressed these concerns in our experiments in four ways. First, we checked sgRNA specificity using publicly available bioinformatic tools (Hsu et al., 2013; Hwang et al., 2013; Sander et al., 2010), selecting the most specific sgRNAs within the region we wished to target. No obvious correlation was detected between the cut rate and the predicted specificity of the sgRNA (Figure 2C; Table S1), with the caveat that we did not screen for mutagenesis at predicted off-target binding sites. Second, we could generate mutant alleles with different sgRNAs and test phenotypes in heteroallelic combination, reducing the likelihood of shared off-target mutations. Third, we successfully used truncated (<20 bp) sgRNAs, which have been shown in cell culture to reduce the likelihood of off-target modifications (Fu et al., 2014). Finally, all lines were outcrossed to wild-type mosquitoes for at least eight generations to reduce co-inheritance of all but the most tightly linked off-target mutations. While these guidelines reduce the likelihood of off-target mutagenesis, there is a need for continued efforts to improve and verify the specificity of all genome-engineering technologies.

### Enhancing the Efficiency of Homology-Directed Repair

In our experiments, insertions and deletions mediated by non-homologous end joining occurred at a much higher frequency than by homology-directed repair. This is similar to what has been observed in *Ae. aegypti* with other genome-editing tools, such as ZFNs (Liesch et al., 2013; McMeniman et al., 2014), and in other organisms, such as *D. melanogaster* (Gratz et al., 2014).

Several approaches have been developed to increase rates of homology-directed repair. These include injections in the background of a DNA ligase 4 mutation (Beumer et al., 2013b, 2013a), or schemes that linearize a double-stranded donor template in vivo. Finally, many laboratories working with *D. melanogaster* have developed transgenic strains that express Cas9 protein under ubiquitous or germline promoters, generally improving the efficiency of mutagenesis and specifically increasing rates of homology-directed repair (Gratz et al., 2014; Ren et al., 2014). It remains to be seen whether transgenic Cas9 delivery or alternative integration approaches can be effectively implemented in *Ae. aegypti*.

We note that we observed a single round of injection that resulted in high (>30%) rates of homology-directed repair but extremely low survival (Table S3). This suggests that we might achieve improvements in insertion efficiency by continuing to modulate the composition of the injection mix. If the rates of homology-directed repair can be sufficiently improved, CRISPR-Cas9 coupled with homology-directed repair will likely prove to be a versatile tool to tag gene products and introduce trans-

genes into specific genomic loci, enabling the study of identified neural circuits and other subsets of cells.

### Conclusion

Precision genome engineering in mosquitoes holds great promise for studies on the genetic basis of behavior (DeGennaro et al., 2013; Liesch et al., 2013; McMeniman et al., 2014), and for genetic strategies to control vector population or disease competence (Alphey, 2014). Ongoing efforts to increase the specificity and efficiency of these technologies is critical to their adaptation as routine techniques, and we believe that the protocols outlined here have met those criteria for the generation of loss-of-function mutations in the mosquito *Ae. aegypti*. Reagents based on CRISPR-Cas9 have been used successfully in organisms from bacteria to primates. This suggests that the techniques described here can likely be adapted to many other non-model organisms, as long as efficient methods for introducing the reagents into the germline and screening for mutations can be developed.

### EXPERIMENTAL PROCEDURES

All laboratory blood-feeding procedures with mice and humans were approved and monitored by The Rockefeller University Institutional Animal Care and Use Committee (11487 and 14756) and Institutional Review Board (LVO-0652). All humans gave their informed consent to participate in mosquito blood-feeding procedures. Detailed procedures are available as [Supplemental Experimental Procedures](#).

#### Cas9 mRNA and Protein

Cas9 mRNA was transcribed from pMLM3613 (Addgene 42251) (Hwang et al., 2013) using mMessage mMachine T7 Ultra Transcription kit (AM1345, Life Technologies). Recombinant Cas9 protein was obtained commercially (CP01, PNA Bio).

#### sgRNA Design and Construction

The sgRNAs were designed by manually searching genomic regions for the presence of PAMs with the sequence NGG, where N is any nucleotide. We required that sgRNA sequences be 17–20 bp in length, excluding the PAM, and contain one or two 5' terminal guanines to facilitate transcription by T7 RNA polymerase. sgRNA sequences were checked for potential off-target binding using the following two web tools: <http://zifit.partners.org/ZiFIT/> and <http://crispr.mit.edu>. See Table S1 for sgRNA sequences and predictions of off-target binding.

#### Extraction of Genomic DNA

Genomic DNA was extracted from individual or pools of mosquitoes using either the DNeasy Blood and Tissue Kit (69581, QIAGEN) or a 96-well-plate extraction protocol (Holleley and Sutcliffe, 2014).

#### Sequencing and Analysis of CRISPR-Cas9-Induced Mutations

A two-step PCR protocol was used to amplify amplicons surrounding the putative CRISPR-Cas9 cut site from genomic DNA of G<sub>0</sub> or G<sub>1</sub> animals using primers in Table S2. Libraries were sequenced on an Illumina MiSeq, aligned to the wild-type reference sequence and examined for the presence of insertions, deletions, or other polymorphisms. Scripts developed for the analysis of this data are available at [https://github.com/bnmthws/crispr\\_indel](https://github.com/bnmthws/crispr_indel).

#### Donor Construction for Homology-Directed Repair

The ssODNs were synthesized as 200-bp Ultramers (Integrated DNA Technologies). Homology arms for plasmid donors were PCR-amplified from LVP-IB12 genomic DNA and cloned with In-Fusion HD cloning (Clontech Laboratories) into PSL1180polyUBdsRED (Addgene 49327) or pSL1180-HR-PUBecFP

(Addgene 47917). Annotated sequences of oligonucleotides and plasmids used for homology-directed repair are available in [Data S2](#).

### Molecular Genotyping of Stable Germline Alleles by PCR

To verify the presence of exogenous sequences inserted by homology-directed repair, or the presence of insertions and deletions, PCR amplicons surrounding the putative cut site were generated from genomic DNA (see [Table S2](#) for primer sequences). Purified amplicons were Sanger sequenced (Genewiz), or used as a template for a restriction digest using BamHI (R0136, New England Biolabs) or PacI (R0547, NEB).

### Statistics

Summary data were plotted using the python packages matplotlib (boxplots) and seaborn (means  $\pm$  95% confidence intervals).

### Genotyping Stable Alleles by Fluorescence

Larvae or pupae were immobilized on a piece of moist filter paper and examined under a dissection microscope (SMZ1500, Nikon) with a fluorescent light source and ECFP and dsRed filter sets.

### ACCESSION NUMBERS

Sequencing data are available from NCBI under Bioproject accession number PRJNA272452.

### SUPPLEMENTAL INFORMATION

Supplemental Information includes Supplemental Experimental Procedures, Data S1 and S2, and three tables and can be found with this article online at <http://dx.doi.org/10.1016/j.celrep.2015.03.009>.

### AUTHOR CONTRIBUTIONS

K.E.K. and B.J.M. designed the study, performed experiments, and analyzed the data. All authors together designed the figures and wrote the paper.

### ACKNOWLEDGMENTS

We thank Rob Harrell and the Insect Transformation Facility/University of Maryland for expert mosquito embryo microinjection, Gloria Gordon and Libby Mejia for mosquito rearing, and members of the L.B.V. laboratory for helpful comments and critiques. We thank Román Corfas and Conor McMeniman for feedback on an earlier version of this paper. This work was supported in part by contract HHSN272200900039C from the National Institute of Allergy and Infectious Diseases and grant UL1 TR000043 from the National Center for Advancing Translational Sciences (NCATS, NIH Clinical and Translational Science Award [CTSA] program). B.J.M. was a Jane Coffin Childs Postdoctoral Fellow and L.B.V. is an investigator of the Howard Hughes Medical Institute.

Received: January 15, 2015

Revised: February 21, 2015

Accepted: February 27, 2015

Published: March 26, 2015

### REFERENCES

- Alphey, L. (2014). Genetic control of mosquitoes. *Annu. Rev. Entomol.* 59, 205–224.
- Aryan, A., Anderson, M.A.E., Myles, K.M., and Adelman, Z.N. (2013a). TALEN-based gene disruption in the dengue vector *Aedes aegypti*. *PLoS ONE* 8, e60082.
- Aryan, A., Anderson, M.A.E., Myles, K.M., and Adelman, Z.N. (2013b). Germ-line excision of transgenes in *Aedes aegypti* by homing endonucleases. *Sci. Rep.* 3, 1603.
- Aryan, A., Myles, K.M., and Adelman, Z.N. (2014). Targeted genome editing in *Aedes aegypti* using TALENs. *Methods* 69, 38–45.
- Bassett, A.R., Tibbit, C., Ponting, C.P., and Liu, J.-L. (2013). Highly efficient targeted mutagenesis of *Drosophila* with the CRISPR/Cas9 system. *Cell Rep.* 4, 220–228.
- Beumer, K.J., Trautman, J.K., Mukherjee, K., and Carroll, D. (2013a). Donor DNA utilization during gene targeting with zinc-finger nucleases. *G3 (Bethesda)* 3, 657–664.
- Beumer, K.J., Trautman, J.K., Christian, M., Dahlem, T.J., Lake, C.M., Hawley, R.S., Grunwald, D.J., Voytas, D.F., and Carroll, D. (2013b). Comparing zinc finger nucleases and transcription activator-like effector nucleases for gene targeting in *Drosophila*. *G3 (Bethesda)* 3, 1717–1725.
- Bhatt, S., Gething, P.W., Brady, O.J., Messina, J.P., Farlow, A.W., Moyes, C.L., Drake, J.M., Brownstein, J.S., Hoen, A.G., Sankoh, O., et al. (2013). The global distribution and burden of dengue. *Nature* 496, 504–507.
- Brinkman, E.K., Chen, T., Amendola, M., and van Steensel, B. (2014). Easy quantitative assessment of genome editing by sequence trace decomposition. *Nucleic Acids Res.* 42, e168.
- Carroll, D. (2014). Genome engineering with targetable nucleases. *Annu. Rev. Biochem.* 83, 409–439.
- Coates, C.J., Jasinskiene, N., Miyashiro, L., and James, A.A. (1998). Mariner transposition and transformation of the yellow fever mosquito, *Aedes aegypti*. *Proc. Natl. Acad. Sci. USA* 95, 3748–3751.
- Dahlem, T.J., Hoshijima, K., Juryne, M.J., Gunther, D., Starker, C.G., Locke, A.S., Weis, A.M., Voytas, D.F., and Grunwald, D.J. (2012). Simple methods for generating and detecting locus-specific mutations induced with TALENs in the zebrafish genome. *PLoS Genet.* 8, e1002861.
- DeGennaro, M., McBride, C.S., Seeholzer, L., Nakagawa, T., Dennis, E.J., Goldman, C., Jasinskiene, N., James, A.A., and Vosshall, L.B. (2013). *orco* mutant mosquitoes lose strong preference for humans and are not repelled by volatile DEET. *Nature* 498, 487–491.
- DePristo, M.A., Banks, E., Poplin, R., Garimella, K.V., Maguire, J.R., Hartl, C., Philippakis, A.A., del Angel, G., Rivas, M.A., Hanna, M., et al. (2011). A framework for variation discovery and genotyping using next-generation DNA sequencing data. *Nat. Genet.* 43, 491–498.
- Doudna, J.A., and Charpentier, E. (2014). Genome editing. The new frontier of genome engineering with CRISPR-Cas9. *Science* 346, 1258096.
- Fu, Y., Sander, J.D., Reyon, D., Cascio, V.M., and Joung, J.K. (2014). Improving CRISPR-Cas nuclease specificity using truncated guide RNAs. *Nat. Biotechnol.* 32, 279–284.
- Gagnon, J.A., Valen, E., Thyme, S.B., Huang, P., Ahkmetova, L., Pauli, A., Montague, T.G., Zimmerman, S., Richter, C., and Schier, A.F. (2014). Efficient mutagenesis by Cas9 protein-mediated oligonucleotide insertion and large-scale assessment of single-guide RNAs. *PLoS ONE* 9, e98186.
- Gratz, S.J., Ukken, F.P., Rubinstein, C.D., Thiede, G., Donohue, L.K., Cummings, A.M., and O'Connor-Giles, K.M. (2014). Highly specific and efficient CRISPR/Cas9-catalyzed homology-directed repair in *Drosophila*. *Genetics* 196, 961–971.
- Holley, C., and Sutcliffe, A. (2014). 2014 Methods in *Anopheles* Research (Centers for Disease Control). Atlanta, GA. <http://www.mr4.org/AnophelesProgram/TrainingMethods.aspx>. Accessed 2/19/2015.
- Hsu, P.D., Scott, D.A., Weinstein, J.A., Ran, F.A., Konermann, S., Agarwala, V., Li, Y., Fine, E.J., Wu, X., Shalem, O., et al. (2013). DNA targeting specificity of RNA-guided Cas9 nucleases. *Nat. Biotechnol.* 31, 827–832.
- Hwang, W.Y., Fu, Y., Reyon, D., Maeder, M.L., Tsai, S.Q., Sander, J.D., Peterson, R.T., Yeh, J.-R.J., and Joung, J.K. (2013). Efficient genome editing in zebrafish using a CRISPR-Cas system. *Nat. Biotechnol.* 31, 227–229.
- Jinek, M., Chylinski, K., Fonfara, I., Hauer, M., Doudna, J.A., and Charpentier, E. (2012). A programmable dual-RNA-guided DNA endonuclease in adaptive bacterial immunity. *Science* 337, 816–821.
- Jinek, M., Jiang, F., Taylor, D.W., Sternberg, S.H., Kaya, E., Ma, E., Anders, C., Hauer, M., Zhou, K., Lin, S., et al. (2014). Structures of Cas9 endonucleases reveal RNA-mediated conformational activation. *Science* 343, 1247997.

- Juneja, P., Osei-Poku, J., Ho, Y.S., Ariani, C.V., Palmer, W.J., Pain, A., and Jiggins, F.M. (2014). Assembly of the genome of the disease vector *Aedes aegypti* onto a genetic linkage map allows mapping of genes affecting disease transmission. *PLoS Negl. Trop. Dis.* *8*, e2652.
- Liesch, J., Bellani, L.L., and Vosshall, L.B. (2013). Functional and genetic characterization of neuropeptide Y-like receptors in *Aedes aegypti*. *PLoS Negl. Trop. Dis.* *7*, e2486.
- Lobo, N.F., Hua-Van, A., Li, X., Nolen, B.M., and Fraser, M.J., Jr. (2002). Germ line transformation of the yellow fever mosquito, *Aedes aegypti*, mediated by transpositional insertion of a piggyBac vector. *Insect Mol. Biol.* *11*, 133–139.
- Lobo, N.F., Clayton, J.R., Fraser, M.J., Kafatos, F.C., and Collins, F.H. (2006). High efficiency germ-line transformation of mosquitoes. *Nat. Protoc.* *1*, 1312–1317.
- McMeniman, C.J., Corfas, R.A., Matthews, B.J., Ritchie, S.A., and Vosshall, L.B. (2014). Multimodal integration of carbon dioxide and other sensory cues drives mosquito attraction to humans. *Cell* *156*, 1060–1071.
- Nene, V., Wortman, J.R., Lawson, D., Haas, B., Kodira, C., Tu, Z.J., Loftus, B., Xi, Z., Megy, K., Grabherr, M., et al. (2007). Genome sequence of *Aedes aegypti*, a major arbovirus vector. *Science* *316*, 1718–1723.
- Peng, Y., Clark, K.J., Campbell, J.M., Panetta, M.R., Guo, Y., and Ekker, S.C. (2014). Making designer mutants in model organisms. *Development* *141*, 4042–4054.
- Ren, X., Sun, J., Housden, B.E., Hu, Y., Roesel, C., Lin, S., Liu, L.-P., Yang, Z., Mao, D., Sun, L., et al. (2013). Optimized gene editing technology for *Drosophila melanogaster* using germ line-specific Cas9. *Proc. Natl. Acad. Sci. USA* *110*, 19012–19017.
- Ren, X., Yang, Z., Xu, J., Sun, J., Mao, D., Hu, Y., Yang, S.-J., Qiao, H.-H., Wang, X., Hu, Q., et al. (2014). Enhanced specificity and efficiency of the CRISPR/Cas9 system with optimized sgRNA parameters in *Drosophila*. *Cell Rep.* *9*, 1151–1162.
- Reyon, D., Tsai, S.Q., Khayter, C., Foden, J.A., Sander, J.D., and Joung, J.K. (2012). FLASH assembly of TALENs for high-throughput genome editing. *Nat. Biotechnol.* *30*, 460–465.
- Sander, J.D., Maeder, M.L., Reyon, D., Voytas, D.F., Joung, J.K., and Dobbs, D. (2010). ZIFIT (Zinc Finger Targeter): an updated zinc finger engineering tool. *Nucleic Acids Res.* *38*, W462–W468.
- Stoddard, B.L. (2014). Homing endonucleases from mobile group I introns: discovery to genome engineering. *Mob. DNA* *5*, 7.
- Timoshevskiy, V.A., Kinney, N.A., deBruyn, B.S., Mao, C., Tu, Z., Severson, D.W., Sharakhov, I.V., and Sharakhova, M.V. (2014). Genomic composition and evolution of *Aedes aegypti* chromosomes revealed by the analysis of physically mapped supercontigs. *BMC Biol.* *12*, 27.
- Wu, T.D., and Nacu, S. (2010). Fast and SNP-tolerant detection of complex variants and splicing in short reads. *Bioinformatics* *26*, 873–881.
- Wu, X., Scott, D.A., Kriz, A.J., Chiu, A.C., Hsu, P.D., Dadon, D.B., Cheng, A.W., Trevino, A.E., Konermann, S., Chen, S., et al. (2014). Genome-wide binding of the CRISPR endonuclease Cas9 in mammalian cells. *Nat. Biotechnol.* *32*, 670–676.